View Online
Dynamic Article Links

Dalton Transactions

Cite this: *Dalton Trans.*, 2011, **40**, 2542

www.rsc.org/dalton

PAPER

SO_2-binding properties of cationic η^6,η^1-NCN-pincer arene ruthenium platinum complexes: spectroscopic and theoretical studies†

Sylvestre Bonnet,[a,b] Joop H. van Lenthe,[c] Hubertus J. J. van Dam,[d] Gerard van Koten[a] and Robertus J. M. Klein Gebbink*[a]

Received 21st October 2010, Accepted 8th December 2010
DOI: 10.1039/c0dt01437k

The SO_2-binding properties of a series of η^6,η^1-NCN-pincer ruthenium platinum complexes (NCN = 2,6-bis[(dimethylamino)methyl]phenyl anion) have been studied by both UV-visible spectroscopy and theoretical calculations. When an electron-withdrawing $[Ru(C_5R_5)]^+$ fragment (R = H or Me) is η^6-coordinated to the phenyl ring of the NCN-pincer platinum fragment (***cf***. **[2]**$^+$ and **[3]**$^+$, see Scheme 1), the characteristic orange coloration (pointing to η^1- SO_2 binding to Pt) of a solution of the parent NCN-pincer platinum complex **1** in dichloromethane upon SO_2-bubbling is not observed. However, when the ruthenium center is η^6-coordinated to a phenyl substituent linked in *para*-position to the carbon-to-platinum bond, *i.e*. complex **[4]**$^+$, the SO_2-binding property of the NCN-platinum center seems to be retained, as bubbling SO_2 into a solution of the latter complex produces the characteristic orange color. We performed theoretical calculations at the MP2 level of approximation and TD-DFT studies, which enabled us to interpret the absence of color change in the case of **[2]**$^+$ as an absence of coordination of SO_2 to platinum. We analyze this absence or weaker SO_2-coordination in dichloromethane to be a consequence of the relative electron-poorness of the platinum center in the respective η^6-ruthenium coordinated NCN-pincer platinum complexes, that leads to a lower binding energy and an elongated calculated Pt–S bond distance. We also discuss the effects of electrostatic interactions in these cationic systems, which also seems to play a destabilizing role for complex $[\mathbf{2}(SO_2)]^+$.

Introduction

In the past decade, considerable attention has been focused on transition metal-based multifunctional molecules, in which several functional units comprising one metal atom are covalently attached to each other.[1–6] By combining spatial proximity and "through-bond" interactions, well-designed covalent assemblies often show new properties or enhanced performances, compared to a mixture of their monometallic constituents. *Para*-substituted NCN-pincer platinum complexes having the general formula [PtX(NCN-4-Z)] (NCN-4-Z = κ^3-[2,6-$(CH_2NMe_2)_2C_6H_2$-4-Z]$^-$; Z is an organic substituent such as NO_2, NH_2, OMe or Me; X = Cl, Br, I) occupy a special position in this field: they are stable and can be easily integrated into polymetallic architectures.[7–9] In addition, they can react reversibly with electrophilic small molecules like I_2 or SO_2, which makes them appealing as color biomarkers[10] or gas sensors.[11,12] In particular, SO_2 has been shown to reversibly bind in η^1-fashion to the platinum atom of, *e.g.*, [PtCl(NCN-4-H)] (**1**, see Scheme 1a) both in the solid state[11] and in solution, giving a bright orange complex $[\mathbf{1}(SO_2)]$ that has been crystallographically characterized.[13] The mechanism of this reaction has been experimentally and theoretically investigated by DFT methods.[14] According to these calculations, SO_2 directly binds to the platinum atom and not to the halide ligand, as was shown to be the case for other platinum complexes,[15,16] nor does it insert into the η^1-Pt–C bond.[17,18]

We recently published the synthesis and characterization of the heterobimetallic, cationic complexes **[2]**$^+$ and **[3]**$^+$ (see Scheme 1b), in which the arene ring of the NCN-pincer platinum fragment is η^1-bonded to the Pt–X unit as well as η^6-coordinated to $[Ru(C_5R_5)]^+$ (R = H or Me).[19] We have also reported on corresponding heteronuclear RuPd complexes.[20,21] In the RuPt-complexes, the

[a]*Organic Chemistry & Catalysis, Debye Institute for Nanomaterial Science, Faculty of Science, Utrecht University, Padualaan 8, 3584, CH Utrecht, The Netherlands*
[b]*Leiden Institute of Chemistry, Gorlaeus Laboratories, Leiden University, PO Box 9502, 2300, RA Leiden, The Netherlands*
[c]*Theoretical Chemistry Group, Debye Institute for Nanomaterial Science, Faculty of Science, Utrecht University, Padualaan 8, 3584, CH Utrecht, The Netherlands*
[d]*Pacific Northwest National Laboratory, P.O. Box 999, Richland, WA, 99352, USA*

† Electronic supplementary information (ESI) available: UV-vis spectra of the dichloromethane solutions before and after SO_2 bubbling; bond distances, angles, electronic parameters, and TD-DFT calculated electronic transitions for complexes **1**, **[2]**Cl and **[4]**Cl; and atomic *x*, *y*, *z* coordinates of all minimized structures. See DOI: 10.1039/c0dt01437k

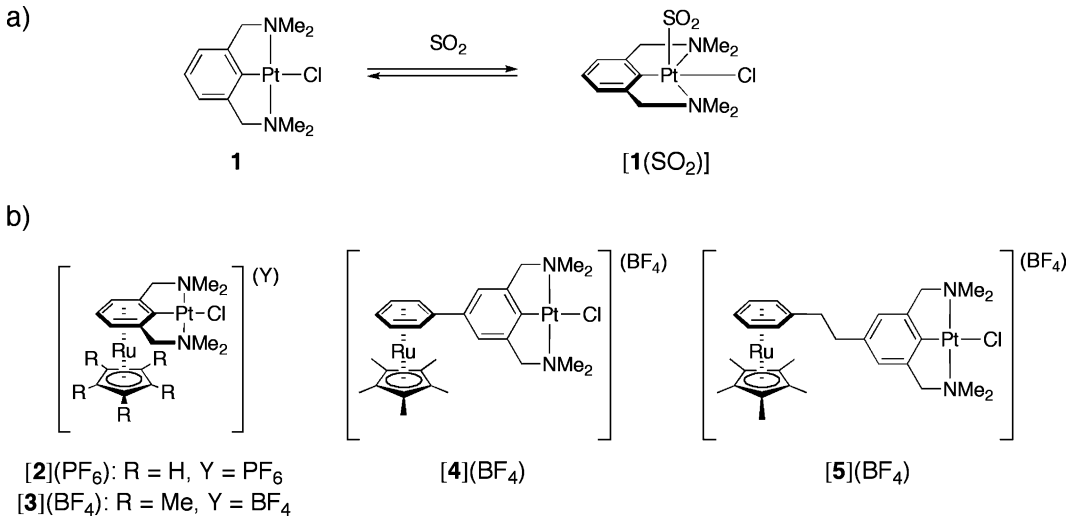

Scheme 1 (a) The reaction between NCN-pincer platinum complex **1** and SO_2, and (b) η^6,η^1-NCN-pincer arene ruthenium platinum complexes used in this study.

platinum center was shown to be less electron-rich than in **1**, which would predict for this metal a decreased nucleophilicity and an enhanced π Lewis acidity. In our initial communication, we mentioned that the SO_2-binding reactivity known for **1** seemed to be quenched for complexes $[\mathbf{2}]^+$ and $[\mathbf{3}]^+$. However, the charge difference between **1** on the one hand, and $[\mathbf{2}]^+$ and $[\mathbf{3}]^+$ on the other hand, hampered direct comparison of their chemical reactivity. The recently synthesized[22] complexes $[\mathbf{4}]^+$ and $[\mathbf{5}]^+$ (see Scheme 1) enable us to draw in this article a more complete picture of how SO_2 binds to η^6,η^1-ruthenium platinum complexes. Upon bubbling SO_2 gas through solutions of $[\mathbf{4}]^+$ and $[\mathbf{5}]^+$ in dichloromethane these complexes do produce an orange color characteristic of the formation of η^1-SO_2 platinum adducts, whereas $[\mathbf{2}]^+$ and $[\mathbf{3}]^+$ do not. We measured by UV-vis spectroscopy these color changes, and benchmarked our spectroscopic data with the data obtained from theoretical calculations to assess in which case coordination to platinum was occurring. Our calculations show that coordination of SO_2 to $[\mathbf{2}]^+$ is theoretically possible, but leads to a 0.1 Å longer Pt–S bond and 21 kJ mol^{-1} weaker binding energy for $[\mathbf{2}]^+$ than for $[\mathbf{4}]^+$. We provide an interpretation of this weakened platinum-SO_2 interaction based on 1) the electron-withdrawing effects of the η^6-coordinated ruthenium fragment ("through bond interaction"), and 2) the destabilizing charge–dipole interactions between the positive charge of the ruthenium center and the dipole moment of the SO_2-coordinated NCN-pincer platinum fragment ("through space interactions").

Experimental part

Spectroscopic study

Dichloromethane solutions (CH_2Cl_2, 10^{-4} M) of **1**, $[\mathbf{2}]PF_6$, $[\mathbf{3}]BF_4$, $[\mathbf{4}]BF_4$ and $[\mathbf{5}]BF_4$ were prepared,[22] and their UV-vis spectra recorded (see Table 1 and Fig. S1†). These solutions were saturated with SO_2 by gentle bubbling during one minute, and the new UV-vis spectra were recorded between 330 and 800 nm.[23]

Table 1 Spectroscopic data before and after saturation of solutions of the compounds in dichloromethane with SO_2 gas

	λ (nm)/ε (cm^{-1} L mol^{-1})	
Complex	Before SO_2-bubbling	After SO_2-bubbling
1[a]	268sh/8000 279/9700 297sh/3700	352/6500 408sh/1700
$[\mathbf{2}](PF_6)$	310/1700	No changes
$[\mathbf{3}](BF_4)$	263sh/10100	No changes
$[\mathbf{4}](BF_4)$	343/15700	348sh/6600 400sh/1900
$[\mathbf{5}](BF_4)$	270sh/10500 284/13600 305sh/4800	353/5900 406sh/1800

[a] According to ref. 36.

Theoretical calculations

For all calculations the SDD basis set with quasi-relativistic MWB pseudopotential was chosen for Pt and Ru atoms, and the 6-31G* basis sets for the other atoms. Complexes $[\mathbf{2}]Cl$, $[\mathbf{4}]Cl$, $[\mathbf{2}(SO_2)]Cl$, and $[\mathbf{4}(SO_2)]Cl$, were optimized in the ground state using Gaussian 2003[24] under the second-order Møller–Plesset perturbation method.[25] For all cationic bimetallic complexes the chloride counter-anion was added to keep the global charge of the molecule neutral. For the SO_2-adducts the Counterpoise method[26] was used in MP2 calculations to avoid the Basis Set Superposition Error (BSSE). In order to check our calculation method the geometry of **1** and $[\mathbf{1}(SO_2)]$ were also minimized, which gave geometries identical as in Zhou's paper.[27]

Natural charges (Q) as defined by the Natural Bond Orbital (NBO) theory,[28] bond indices (BI),[29] local dipoles q^1 as defined by the Distributed Multipole Analysis (DMA),[30] as well as the SO_2-binding energies calculated under the MP2 approximation using

the Counterpoise method,[26] were calculated using the GAMESS-UK electronic structure package.[31]

The first singlet electronic transitions for the MP2-minimized geometries of complexes for [**1**(SO_2)], [**2**(SO_2)]Cl, and [**4**(SO_2)]Cl (λ_{ex} > 330 nm), were calculated by the TD-DFT/B3LYP method[32] as implemented in the NWChem *ab initio* calculation package.[33] For comparison purposes the electronic transitions for complexes **1**, [**2**]Cl, and [**4**]Cl (λ_{ex} > 250 nm) were also calculated using the same method. Electron density difference plots in Fig. 2 were realized using NWChem[34] and CCP1GUI[35] adapted by H. van Dam.

Results

Upon saturation with SO_2 gas, dichloromethane solutions of complexes **1**, [**4**]$^+$ and [**5**]$^+$ turn bright orange, whereas solutions of [**2**]$^+$ and [**3**]$^+$ remain colorless. Table 1 shows the main features of the UV-vis spectra before and after reaction with SO_2 (see also Fig. S1 and Fig. S2†). The UV-vis spectra of SO_2-saturated solutions of [**4**]$^+$ and [**5**]$^+$ closely resemble those of complex [**1**(SO_2)], with an absorption maximum around 350 nm and a shoulder around 400 nm. The latter is responsible for the orange color of the solution. By contrast, for [**2**]$^+$ and [**3**]$^+$ no characteristic absorption bands were observed above 330 nm.

Geometry minimizations of the SO_2-adducts [**2**(SO_2)]Cl and [**4**(SO_2)]Cl under the MP2 approximation using Counterpoise led to local minima in all cases. The minimized geometries are shown in Fig. 1, and characteristic bond distances and angles are given in Table 2. In the minimized geometries of complexes [**2**]Cl and [**4**]Cl the NCN-pincer fragment is characterized by a *pseudo*-C_2 axis co-linear to the Pt–C_{ipso} bond.[37] This is consistent with the geometry of [**2**]BF_4 observed experimentally in the solid state.[22] By contrast, the geometries found for [**2**(SO_2)]Cl and [**4**(SO_2)]Cl are characterized by a plane of symmetry for the NCN-pincer fragment. This plane is perpendicular to the plane of the pincer arene ring, and comprises S, Pt, C_{ipso} and C_{para}. The same type of geometry was observed in the crystal structure[13] and in the calculated structure[27] of [**1**(SO_2)]. As reported by Zhou *et al.* the SO_2-adducts are *trans*, with the orientation of the OSO bending away from the chloride anion coordinated to platinum.[27]

As shown in Table 2 the Pt–S bond distance is found much longer in [**2**(SO_2)]Cl (2.802 Å) than in [**4**(SO_2)]Cl (2.705 Å), which in turn is longer than in [**1**(SO_2)] (2.612 Å). Natural charges (Q)[28] and local dipoles [30] q^1 represent two different ways to evaluate the charge distribution in the molecules (see Table 3 and Supplementary Information†). Thus, although the positive charge on platinum slightly decreases following the series [**1**(SO_2)], [**4**(SO_2)]Cl, [**2**(SO_2)]Cl, the local dipole q^1 is twice as large for [**2**(SO_2)]Cl as for [**1**(SO_2)] and [**4**(SO_2)]Cl. The platinum atom is hence much more polarized in [**2**(SO_2)]Cl.

Table 2 Bond distance (Å) and angles (°) in the MP2-minimized geometries of [**2**(SO_2)]Cl and [**4**(SO_2)]Cl. For comparison purposes the corresponding parameters in the calculated and experimental structure of [**1**(SO_2)] are also given

Parameter	[**2**(SO_2)]Cl (MP2)[a]	[**4**(SO_2)]Cl (MP2)[a]	[**1**(SO_2)] (MP2)[a]	[**1**(SO_2)] (X-ray)[b]
Pt–S	2.802	2.705	2.612	2.570(1)
S–O	1.493	1.496	1.490	1.451(4)
Pt–Cl	2.405	2.416	2.424	2.409(1)
Pt–C_{ipso}	1.917	1.925	1.932	1.934(4)
Pt–N	2.102	2.097	2.103	2.094(3)
Cl–Pt–C_{ipso}	173.18	170.97	168.58	173.14(11)
N–Pt–C_{ipso}	82.68	81.88	81.792	81.95(13)
O–S–Pt	101.38	102.405	103.46	103.22(12)
O–S–O	116.78	116.52	116.192	113.4(2)
C_{ortho}–C_{ipso}–Pt–N	1.78	3.55	4.05	2.1(3)

[a] From own MP2 calculations; [b] according to ref. 38.

Table 3 Electronic and energetic parameters for the MP2-minimized geometries of free SO_2, [**2**(SO_2)]Cl, and [**4**(SO_2)]Cl. For comparison purposes the values for [**1**(SO_2)] are also given

Parameter	SO_2	[**2**(SO_2)]Cl	[**4**(SO_2)]Cl	[**1**(SO_2)]
Q(Pt)	—	0.610	0.612	0.620
q^1(Pt)	—	1.04	0.501	0.482
Q(Cl)	—	–0.638	–0.650	–0.659
q^1(Cl)	—	0.693	0.681	0.672
Q(C_{ipso})	—	–0.191	–0.187	–0.190
q^1(C_{ipso})	—	1.06	0.822	0.847
Q(S)	1.536	1.534	1.520	1.519
q^1(S)	0.757	0.737	0.748	0.794
Q(O)	–0.768	–0.852	–0.859	–0.873
q^1(O)	0.191	0.202	0.215	0.211
BI(Pt–C_{ipso})	—	0.872	0.819	0.820
BI(Pt–Cl)	—	0.974	0.934	0.922
BI(Pt–S)	—	0.371	0.432	0.490
BI(S–O)	1.758	1.536	1.524	1.511
Binding energy kJ mol^{-1}	—	75	96	101

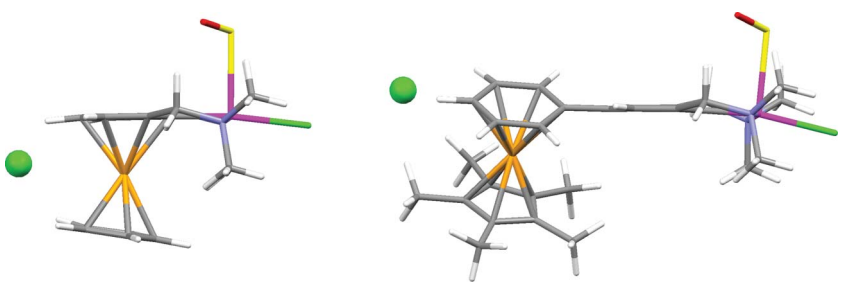

Fig. 1 Caped stick side view of the MP2-minimized geometries of complexes [**2**(SO_2)]Cl (left) and [**4**(SO_2)]Cl (right). The non-coordinated chloride counter-anion is represented as a sphere.

Table 4 Calculated electronic transitions for complexes [**1**(SO_2)], [**2**(SO_2)]Cl, and [**4**(SO_2)]Cl. Only the most intense transition ($f > 0.01$) with $\lambda > 300$ nm are given

	Calculated transitions		
Complex	E (eV)	λ (nm)	f
[**1**(SO_2)]	2.64	470	0.0184
	3.45	360	0.1027
	4.03	308	0.0167
[**2**(SO_2)]Cl	2.62	474	0.0121
	3.31	375	0.0793
	3.44	361	0.0376
[**4**(SO_2)]Cl	2.48	500	0.0293
	3.11	399	0.0107
	3.36	369	0.1108

The MP2 method with Counterpoise[26] was used to calculate the binding energies of SO_2 to [**1**], [**2**]Cl and [**4**]Cl according to equations (1), (2) and (3):

$$[\mathbf{1}]_{(g)} + SO_{2(g)} \rightleftarrows [\mathbf{1}(SO_2)]_{(g)}\ \Delta E_1 = -101\ \text{kJ mol}^{-1} \quad (1)$$

$$[\mathbf{2}]Cl_{(g)} + SO_{2(g)} \rightleftarrows [\mathbf{2}(SO_2)]Cl_{(g)}\ \Delta E_2 = -75\ \text{kJ mol}^{-1} \quad (2)$$

$$[\mathbf{4}]Cl_{(g)} + SO_{2(g)} \rightleftarrows [\mathbf{4}(SO_2)]Cl_{(g)}\ \Delta E_4 = -96\ \text{kJ mol}^{-1} \quad (3)$$

ΔE_2 was found 26 kJ mol^{-1} lower than ΔE_1, whereas ΔE_4 was found only 5 kJ mol^{-1} lower.

Calculated spectra

The most relevant electronic transitions for complexes [**2**(SO_2)]Cl and [**4**(SO_2)]Cl (*i.e.*, those with a oscillator strength larger than 0.01) were calculated by TD-DFT (see Table 4 and Fig. 2). For [**4**(SO_2)]Cl two weak transitions were found in the visible region (499.7 and 398.8 nm), and a strong one in the UV region (369.2 nm). These transitions are similar to the transitions found by TD-DFT at 469.8 and 359.5 nm for complex [**1**(SO_2)] (see Fig. 2). For [**2**(SO_2)]Cl similar transitions were found at 473.5 nm and 374.8 nm. The transition in the visible region is characterized by an oscillator strength of 0.0121, which is comparable to the oscillator strength of the transitions in the visible for [**1**(SO_2)] (0.0184) and for [**4**(SO_2)]Cl (0.0293). These results predict an orange color for complex [**2**(SO_2)]Cl as well.

Discussion

In a recent article, Zhou *et al.* demonstrated[27] that DFT was poorly adapted to describe the weak interaction between NCN-pincer platinum complexes and SO_2, which consists in a large part of dispersion forces. They showed that MP2 calculation with BSSE correction methods were better adapted for such molecules, and give in the case of complexes **1** and [**1**(SO_2)] geometries that are very close to the available experimental data.[36,38] Based on this work we used the same calculation method to investigate how SO_2 could bind to complexes [**2**]$^+$ and [**4**]$^+$, and for consistency issues we repeated Zhou's calculation on complexes **1** and [**1**(SO_2].

It is relatively straightforward to interpret the orange color observed when [**4**]$^+$ and [**5**]$^+$ are put into contact with SO_2 as the characteristic color of [**4**(SO_2)]$^+$ and [**5**(SO_2)]$^+$, respectively (see Scheme 2). The experimental absorption maxima correspond well to that of [**1**(SO_2)],[14,27,36,39–41] and the band found at 500 nm by TD-DFT calculation for complex [**4**(SO_2)]Cl is similar to that found at 470 nm for [**1**(SO_2)]. In addition, the electron-richness of the platinum center in [**4**]$^+$ and [**5**]$^+$ is only slightly modified compared to **1**,[22] which would predict a comparable nucleophilicity for [**4**]$^+$, [**5**]$^+$, and **1**.

^{195}Pt NMR and electrochemical studies have shown that complexes [**2**]$^+$ and [**3**]$^+$ have a dramatically reduced electron-density on platinum, compared to **1**, [**5**]$^+$ and [**4**]$^+$.[22] Consequently [**2**]$^+$ and [**3**]$^+$ are expected to be less reactive towards electrophiles like SO_2. Accordingly, we interpret the absence of orange color when [**2**]$^+$ and [**3**]$^+$ are put in presence of SO_2 as an absence of SO_2-coordination to the platinum center (see Scheme 2). However, such an assumption requires additional argumentation, as it might be questioned whether species that we cannot see experimentally, actually do form. For example, the presence of an η^6-coordinated ruthenium center might shift hypsochromically the highest electronic transitions of a hypothetical SO_2-adduct of complex [**2**]$^+$ or [**3**]$^+$, which would hamper its detection by UV-vis spectroscopy. Thus, we performed theoretical calculations in order to support our interpretation.

The local minimum found for [**2**(SO_2)]Cl shows that this SO_2-adduct might also be formed. Its theoretical absorption spectrum,

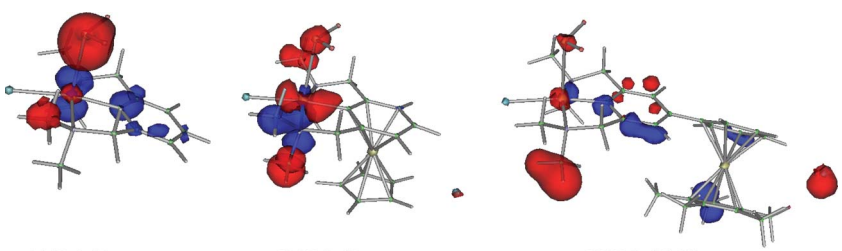

Fig. 2 From left to right: electron density difference plot for the electronic transition in the visible region of complexes [**1**(SO_2)], [**2**(SO_2)]Cl, and [**4**(SO_2)]Cl, according to TD-DFT calculations. Blue lobes correspond to region of depleted electron density in the excited state, red lobes to increased electron density in the excited state.

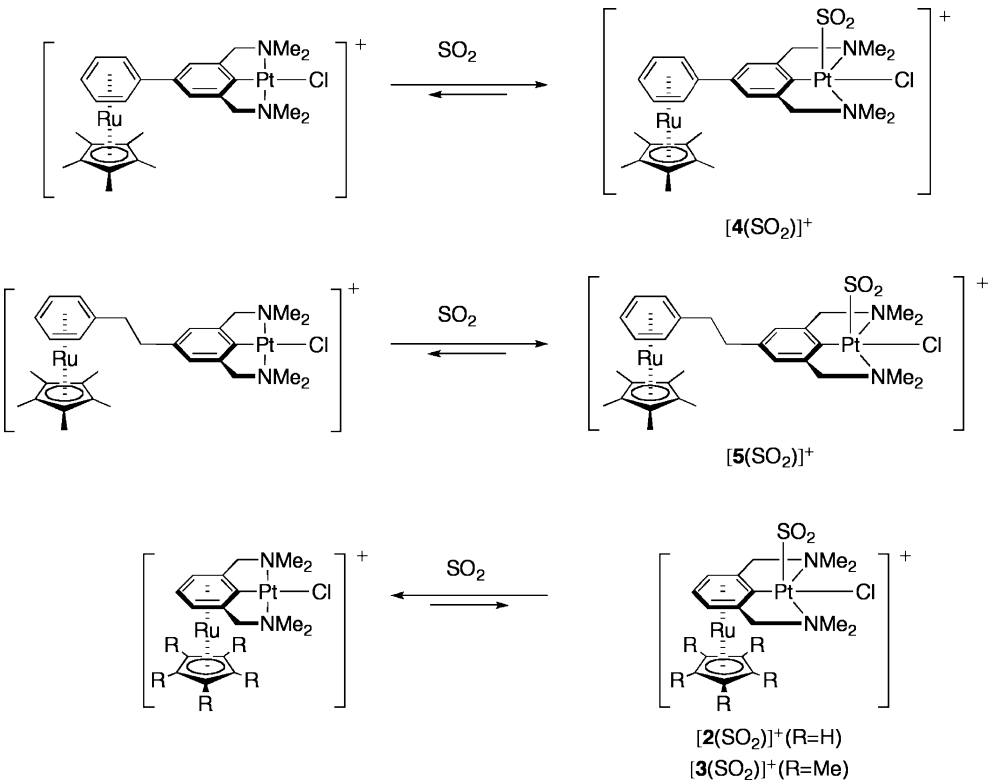

Scheme 2 SO_2-binding on ruthenium-modified NCN-platinum pincer complexes $[\mathbf{2}]^+$–$[\mathbf{5}]^+$.

calculated using TD-DFT, gives electronic transitions at 474 nm, 375 and 361 nm, which predicts a red color for this complex. Considering that these bands are not experimentally observed, we can reasonably conclude that complex $[\mathbf{2}(SO_2)]^+$ does not form in the conditions where $[\mathbf{1}(SO_2)]$ and $[\mathbf{4}(SO_2)]^+$ do. There is hence a specific lack of platinum-based nucleophilicity for structures of the type $[\mathbf{2}]^+$ and $[\mathbf{3}]^+$.

Considering that the four complexes $[\mathbf{2}]^+$–$[\mathbf{5}]^+$ are all positively charged, the cationic nature of complexes $[\mathbf{2}]^+$ and $[\mathbf{3}]^+$ cannot be regarded as the reason for such a reduced nucleophilicity of the platinum center. In order to understand why $[\mathbf{2}(SO_2)]^+$ does not form whereas $[\mathbf{1}(SO_2)]$ and $[\mathbf{4}(SO_2)]^+$ do, we calculated the binding energy of SO_2, *i.e.*, the difference in MP2 energy between each SO_2 adduct and its molecular components (equilibria (1), (2) and (3)). In the case of equilibrium (3) the calculated binding energy is very close to that calculated for (1), which is consistent with our experimental observation of $[\mathbf{4}(SO_2)]^+$. For equilibrium (2) the binding energy is found 26 kJ mol^{-1} lower than for equilibria (1), which might be large enough to explain the different reactivity of $[\mathbf{2}]^+$ and **1**. Earlier studies showed that although the DFT-calculated binding energy was relatively large (ΔE_a = 80 kJ mol^{-1}) for [PtI(NCN–H)]),[14] the experimental binding enthalpy was much weaker (ΔH = –36.6 kJ mol^{-1}), which has been interpreted in terms of solvent effects. Solvent effects might indeed play a significant role considering the importance of dipole moments in the binding of SO_2 to platinum (see below), and the probable formation of an ion pair in dichloromethane for the bimetallic compounds. In addition, the entropy variation was found negative and relatively large for this analog of complex **1** (ΔS = –104 J K^{-1} mol^{-1}), which leads to a small value for the experimental Gibbs free energy variation (ΔG = –5.5 kJ mol^{-1}). Considering that solvents and entropy effects might play similar roles for the binding of SO_2 to **1**, $[\mathbf{2}]^+$, and $[\mathbf{4}]^+$, the loss of 26 kJ mol^{-1} of binding energy might be large enough to result in a very low or even slightly positive Gibbs free energy variation ΔG for equilibrium (2), which would be detrimental to the formation of $[\mathbf{2}(SO_2)]^+$.

One could ask whether such modification of the SO_2-binding energy results from "through bond" interactions, where the electron-withdrawing properties of the $[Ru(C_5R_5)]^+$ fragment are communicated to the platinum center through the bridging ligand,[42,43] or whether the mere presence of a positive charge close to the platinum metal would change substantially its electrostatic environment, hence its coordination properties, which would correspond to "through-space" interactions between the two metals centers.

It is possible to interpret the difference in reactivity between **1**, $[\mathbf{2}]^+$ and $[\mathbf{4}]^+$ in terms of orbital energy. It has been shown[14] that η^1-coordination of SO_2 to the platinum center in **1** takes place in a single step, without intermediate halide-bound SO_2 adduct.[15] Direct electrophilic attack of SO_2 is promoted by the interaction between the high-lying, filled d_{z^2} and d_{xz} orbitals centered on platinum, and the HOMO and LUMO of SO_2.[27,36] The strong electron-withdrawing properties of the η^6-coordinated $[Ru(C_5R_5)]^+$ fragment in [**2**]Cl induces an increased positive charge on platinum compared to **1**, hence a lowering of the energy level of the Pt-centered d_{z^2} and d_{xz} filled orbitals (–9.43 eV and –7.87 eV, respectively, in [**1**], *vs.* –10.19 eV and –9.36 eV in [**2**]Cl). As a result, the interaction with the LUMO of SO_2 is decreased in $[\mathbf{2}(SO_2)]$Cl, which diminishes the bond index BI(Pt–S), (0.37 *vs.* 0.49), elongates the Pt–S bond distance (2.80 *vs.* 2.61 Å),

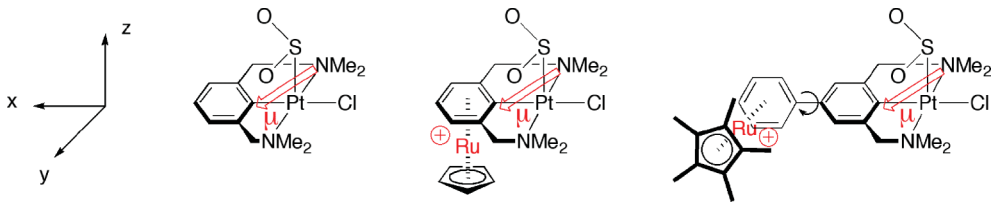

Fig. 3 Charge–dipole interactions in SO_2 adducts of **1**, $[\mathbf{2}]^+$ and $[\mathbf{4}]^+$ (from left to right). The red arrows represent, for each complex, the dipole moment of the NCN-platinum fragment (to which SO_2 is coordinated), and by convention the dipole goes towards the positive charges.

and diminishes the binding energy of SO_2 (75 *vs.* 101 kJ mol^{-1}), compared to $[\mathbf{1}(SO_2)]$.

The difference in reactivity between **[2]**Cl and **1** can also be explained in terms of charge transfer: in the SO_2 adducts the positive NBO charge on platinum is much higher (~ 0.61) than in the complexes without SO_2 (~ 0.53, see Table S2†) because of back-donation from the d_z2 and d_xz filled orbitals, into the LUMO of SO_2. As the electron-withdrawing effect of the ruthenium fragment on platinum increases along the series **1**, $[\mathbf{5}]^+$, $[\mathbf{4}]^+$, $[\mathbf{3}]^+$, $[\mathbf{2}]^+$,[22] the platinum atom becomes more and more positively charged, and back-donation diminishes along this series. The absolute value of the difference in NBO charge between each platinum complex and its SO_2-adduct goes down along the series **1**, $[\mathbf{4}]^+$, $[\mathbf{2}]^+$ ($\Delta Q(Pt)$ = 0.105, 0.084, and 0.065, respectively; see Tables 3 and Table S2†). Binding to SO_2 becomes weaker accordingly, and the Pt–S bond distance increases [d(Pt–S) = 2.61, 2.71 and 2.80 Å, respectively].

As far as electrostatics are concerned, dipoles also play an important role in the modified reactivity of $[\mathbf{2}]^+$ because both platinum and sulfur are highly polarisable elements. The high NBO charge borne by the sulfur atom in free SO_2 [Q(S) = 1.536], and the positive partial charge on platinum in complex **1** [Q(Pt) = 0.515] are not expected to favor electrostatic interaction between these two molecules.[44] However, dipole–dipole interactions between the dipole moment of SO_2 and that of complex **1**, as well as polarization of the platinum center in **1** by the approaching SO_2 molecule,[45] might both explain why attractive interactions exist, which finally lead to η^1-binding. As already noticed in Zhou's work,[27] in SO_2-adducts the dipole of the η^1-bonded SO_2 is found anti-parallel to the dipole of the NCN-pincer fragment. Thus, as Q(Cl) ≈ –0.65 is three times larger than $Q(C_{ipso})$ = –0.19, the coordination sphere of platinum generates a local dipole moment aligned with the *x* axis on Fig. 3. In $[\mathbf{1}(SO_2)]$, the total dipole moment of the complex is in its average plane of symmetry (the *xz* plane in Fig. 3), making an angle $\alpha = 55.6°$ with the *x* axis.[46] Upon η^6-coordination of $[Ru(C_5H_5)]^+$ (complex $[\mathbf{2}(SO_2)]$Cl) a positive charge is introduced precisely in this plane, with the dipole moment of the [PtCl(NCN–H)(SO_2)] fragment pointing towards it. The resulting charge–dipole interaction is destabilizing for complex $[\mathbf{2}(SO_2)]$Cl.[47] Such analysis corresponds to a "field effect", where the presence of a positive charge in the close neighborhood of the platinum center generates an electrostatic field that modifies its reactivity.

In complex $[\mathbf{4}(SO_2)]$Cl the positively charged ruthenium center is further from the platinum atom than in $[\mathbf{2}(SO_2)]$Cl [d(Ru–Pt) = 7.66 Å *vs.* 3.69 Å, respectively]; and it is out of the plane of symmetry of the pincer fragment. Both geometric features reduce the destabilizing charge–dipole interaction in complex $[\mathbf{4}(SO_2)]$Cl compared to complex $[\mathbf{2}(SO_2)]$Cl. In addition, the electron-withdrawing effect of the ruthenium fragment is diminished compared to **[2]**Cl, as $[RuCp^*]^+$ is η^6-coordinated to the second arene ring (the d_z2 and d_xz orbitals in **[4]**Cl have an energy of –10.09 and -8.35 eV, respectively). The reduced "through bond" and "through space" interactions between the two metal centers lead to a calculated SO_2-binding energies that is comparable for $[\mathbf{4}(SO_2)]$Cl and for $[\mathbf{1}(SO_2)]$ (ΔE_{SO_2} = –5 kJ mol^{-1}), whereas $[\mathbf{2}(SO_2)]$Cl is much less stable (ΔE_{SO_2} = –26 kJ mol^{-1}).

Qualitatively, the analysis made for $[\mathbf{2}(SO_2)]^+$ also stands for $[\mathbf{3}(SO_2)]^+$, as the geometry of both complexes is rigid, and the intermetallic distance is short. Similarly, the analysis made for $[\mathbf{4}(SO_2)]^+$ also stands for $[\mathbf{5}(SO_2)]^+$, as the positive charge in $[\mathbf{5}(SO_2)]^+$ is far away from the platinum center (d(Ru–Pt) is 10.2 Å in the *trans*-conformation of the ethyl bridge), and out of the symmetry plane of the SO_2-pincer adduct. Overall, destabilizing "through space" interactions are small in $[\mathbf{4}(SO_2)]^+$ and $[\mathbf{5}(SO_2)]^+$, and large in $[\mathbf{2}(SO_2)]^+$ and $[\mathbf{3}(SO_2)]^+$.

Conclusion

Spectroscopic data and theoretical calculations show that complexes $[\mathbf{2}]^+$ and $[\mathbf{4}]^+$ have a different reactivity towards SO_2: the former does not bind SO_2, whereas the latter has the same reactivity as parent complex **1**. According to MP2 calculations the SO_2-binding energy decreases down the series $[\mathbf{1}(SO_2)]$, $[\mathbf{4}(SO_2)]$Cl, $[\mathbf{2}(SO_2)]$Cl. Based on these calculations, we interpret the effects of η^6-coordination of the $[Ru(C_5R_5)]^+$ fragment to the bridging ligand as a combination of "through bond" and "through space" interactions. On the one hand, the electron density on platinum is reduced in complex **[2]**Cl, *i.e.*, the positive charge on platinum is increased, because of the electron-withdrawing properties of the η^6-coordinated ruthenium fragment. As a consequence, the energy level of the platinum-centered d orbitals is lowered, which leads to a lower nucleophilicity of the platinum center ("through bond" interactions). However, the positive charge borne by the ruthenium fragment is placed near the platinum center, which generates unfavorable charge–dipole interactions for the corresponding SO_2 adduct ("through space" interactions). For the binding of SO_2 to $[\mathbf{2}]^+$ both effects are strong, whereas for the binding to $[\mathbf{4}]^+$ both effects are weak. We assume that the results obtained for $[\mathbf{2}]^+$ and $[\mathbf{4}]^+$ qualitatively apply to $[\mathbf{3}]^+$ and $[\mathbf{5}]^+$, respectively. Thus, for $[\mathbf{2}]^+$ and $[\mathbf{3}]^+$, where a single arene ring is η^6- and η^1-coordinated to two different metals, the SO_2-adducts $[\mathbf{2}(SO_2)]^+$ and $[\mathbf{3}(SO_2)]^+$ are destabilized and do not form in the experimental conditions. For $[\mathbf{4}]^+$ and $[\mathbf{5}]^+$, where the two metal centers are η^6- and η^1-bonded to two different arene rings, both effects are diminished, and their SO_2-adducts $[\mathbf{4}(SO_2)]^+$ and $[\mathbf{5}(SO_2)]^+$ do form, similarly to $[\mathbf{1}(SO_2)]$.

Acknowledgements

We gratefully acknowledge the support of this research by Utrecht University and the NRSC-Catalysis program. This work was supported in part by the Stichting Nationale Computerfaciliteiten (National Computing Facilities Foundation in The Netherlands, NCF) for the use of supercomputer facilities.

References

1 I. M. Dixon, J.-P. Collin, J.-P. Sauvage, F. Barigelletti and L. Flamigni, *Angew. Chem., Int. Ed.*, 2000, **39**, 1292.
2 L. Flamigni, E. Baranoff, J.-P. Collin and J.-P. Sauvage, *Chem.–Eur. J.*, 2006, **12**, 6592.
3 P. de Hoog, C. Boldron, P. Gamez, K. Sliedregt-Bol, I. Roland, M. Pitié, R. Kiss, B. Meunier and J. Reedijk, *J. Med. Chem.*, 2007, **50**, 3148.
4 H. P. Dijkstra, C. A. Kruithof, N. Ronde, R. van de Coevering, D. J. Ramon, D. Vogt, G. P. M. van Klink and G. van Koten, *J. Org. Chem.*, 2003, **68**, 675.
5 J. Wang, H. Li, N. Guo, L. Li, C. L. Stern and T. J. Marks, *Organometallics*, 2004, **23**, 5112.
6 B. M. J. M. Suijkerbuijk and R. J. M. Klein Gebbink, *Angew. Chem., Int. Ed.*, 2008, **47**, 7396.
7 H. P. Dijkstra, M. Albrecht, S. Medici, G. P. M. van Klink and G. van Koten, *Adv. Synth. Catal.*, 2002, **344**, 1135.
8 H. P. Dijkstra, M. D. Meijer, J. Patel, R. Kreiter, G. P. M. van Klink, M. Lutz, A. L. Spek, A. J. Canty and G. van Koten, *Organometallics*, 2001, **20**, 3159.
9 H. P. Dijkstra, P. Steenwinkel, D. M. Grove, M. Lutz, A. L. Spek and G. van Koten, *Angew. Chem., Int. Ed.*, 1999, **38**, 2185.
10 G. Guillena, K. M. Halkes, G. Rodriguez, G. D. Batema, G. van Koten and J. P. Kamerling, *Org. Lett.*, 2003, **5**, 2021.
11 M. Albrecht, M. Lutz, A. L. Spek and G. van Koten, *Nature*, 2000, **406**, 970.
12 M. Albrecht and G. van Koten, *Adv. Mater.*, 1999, **11**, 171.
13 J. Terheijden, G. van Koten, W. P. Mul, D. J. Stufkens, F. Muller and C. H. Stam, *Organometallics*, 1986, **5**, 519.
14 M. Albrecht, R. A. Gossage, U. Frey, A. W. Ehlers, E. J. Baerends, A. E. Merbach and G. van Koten, *Inorg. Chem.*, 2001, **40**, 850.
15 M. R. Snow and J. A. Ibers, *Inorg. Chem.*, 1973, **14**, 224.
16 M. R. Snow, J. McDonald, F. Basolo and J. A. Ibers, *J. Am. Chem. Soc.*, 1972, **94**, 2526.
17 F. Faraone, R. Pietropa, S. Sergi and L. Silvestr, *J. Organomet. Chem.*, 1972, **34**, C55.
18 F. Faraone, L. Silvestro, S. Sergi and R. Pietropa, *J. Organomet. Chem.*, 1972, **46**, 379.
19 S. Bonnet, M. Lutz, A. L. Spek, G. van Koten and R. J. M. Klein Gebbink, *Organometallics*, 2008, **27**, 159.
20 S. Bonnet, J. H. van Lenthe, M. Siegler, A. L. Spek, G. van Koten and R. J. M. Klein Gebbink, *Organometallics*, 2009, **28**, 2325.
21 S. Bonnet, M. Lutz, A. L. Spek, G. van Koten and R. J. M. Klein Gebbink, *Organometallics*, 2010, **29**, 1157.
22 S. Bonnet, M. A. Siegler, M. Lutz, A. L. Spek, G. van Koten and R. J. M. Klein Gebbink, *Eur. J. Inorg. Chem.*, 2010, 4667.
23 Below 330 nm the absorption band of free SO_2 hides the absorption bands of the complexes.
24 M. J. Frisch, G. W. Trucks, H. B. Schlegel, G. E. Scuseria, M. A. Robb, J. R. Cheeseman, J. A. Montgomery, Jr., T. Vreven, K. N. Kudin, J. C. Burant, J. M. Millam, S. S. Iyengar, J. Tomasi, V. Barone, B. Mennucci, M. Cossi, G. Scalmani, N. Rega, G. A. Petersson, H. Nakatsuji, M. Hada, M. Ehara, K. Toyota, R. Fukuda, J. Hasegawa, M. Ishida, T. Nakajima, Y. Honda, O. Kitao, H. Nakai, M. Klene, X. Li, J. E. Knox, H. P. Hratchian, J. B. Cross, V. Bakken, C. Adamo, J. Jaramillo, R. Gomperts, R. E. Stratmann, O. Yazyev, A. J. Austin, R. Cammi, C. Pomelli, J. Ochterski, P. Y. Ayala, K. Morokuma, G. A. Voth, P. Salvador, J. J. Dannenberg, V. G. Zakrzewski, S. Dapprich, A. D. Daniels, M. C. Strain, O. Farkas, D. K. Malick, A. D. Rabuck, K. Raghavachari, J. B. Foresman, J. V. Ortiz, Q. Cui, A. G. Baboul, S. Clifford, J. Cioslowski, B. B. Stefanov, G. Liu, A. Liashenko, P. Piskorz, I. Komaromi, R. L. Martin, D. J. Fox, T. Keith, M. A. Al-Laham, C. Y. Peng, A. Nanayakkara, M. Challacombe, P. M. W. Gill, B. G. Johnson, W. Chen, M. W. Wong, C. Gonzalez and J. A. Pople, *GAUSSIAN 03 (Revision B.03)*, Gaussian, Inc., Wallingford, CT, 2004.
25 M. J. Frisch, M. Headgordon and J. A. Pople, *Chem. Phys. Lett.*, 1990, **166**, 275.
26 F. B. van Duijneveldt, J. G. C. M. van Duijneveldt-van de Rijdt and J. H. van Lenthe, *Chem. Rev.*, 1994, **94**, 1873.
27 X. Zhou, Q. H. Pan, M. X. Li, B. H. Xia and H. X. Zhang, *THEOCHEM*, 2007, **822**, 65.
28 A. E. Reed, L. A. Curtiss and F. Weinhold, *Chem. Rev.*, 1988, **88**, 899.
29 O. G. Stradella, H. O. Villar and E. A. Castro, *Theor. Chim. Acta*, 1986, **70**, 67.
30 A. J. Stone and M. Alderton, *Mol. Phys.*, 1985, **56**, 1047.
31 M. F. Guest, I. J. Bush, H. J. J. van Dam, P. Sherwood, J. M. H. Thomas, J. H. van Lenthe, R. W. A. Havenith and J. Kendrick, *Mol. Phys.*, 2005, **103**, 719.
32 M. E. Casida, C. Jamorski, K. C. Casida and D. R. Salahub, *J. Chem. Phys.*, 1998, **108**, 4439.
33 M. Valiev, E. J. Bylaska, N. Govind, K. Kowalski, T. P. Straatsma, H. J. J. van Dam, D. Wang, J. Nieplocha, E. Apra, T. L. Windus and W. A. de Jong, *Comput. Phys. Commun.*, 2010, **181**, 1477.
34 E. J. Bylaska, W. A. de Jong, K. Kowalski, T. P. Straatsma, M. Valiev, D. Wang, E. Aprà, T. L. Windus, S. Hirata, M. T. Hackler, Y. Zhao, P.-D. Fan, R. J. Harrison, M. Dupuis, D. M. A. Smith, J. Nieplocha, V. Tipparaju, M. Krishnan, A. A. Auer, M. Nooijen, E. Brown, G. Cisneros, G. I. Fann, H. Früchtl, J. Garza, K. Hirao, R. Kendall, J. Nichols, K. Tsemekhman, K. Wolinski, J. Anchell, D. Bernholdt, P. Borowski, T. Clark, D. Clerc, H. Dachsel, M. Deegan, K. Dyall, D. Elwood, E. Glendening, M. Gutowski, A. Hess, J. Jaffe, B. Johnson, J. Ju, R. Kobayashi, R. Kutteh, Z. Lin, R. Littlefield, X. Long, B. Meng, T. Nakajima, S. Niu, M. Rosing, G. Sandrone, M. Stave, H. Taylor, G. Thomas, J. van Lenthe, A. Wong and Z. Zhang, *NWChem, a computational chemistry package for parallel computers*, version 5.0 (2006), Pacific Northwest National Laboratory, Richland, Washington USA 99352–0999, A modified version.
35 The CCP1GUI project: http://www.cse.scitech.ac.uk/ccg/software/ccp1gui/ (2008).
36 M. Albrecht, R. A. Gossage, M. Lutz, A. L. Spek and G. van Koten, *Chem.–Eur. J.*, 2000, **6**, 1431.
37 We also recently published the DFT-minimized structures of complexes **1** and $[\mathbf{2}]^+$–$[\mathbf{5}]^+$, see ref. 22.
38 M. Albrecht, M. Lutz, A. M. M. Schreurs, E. T. H. Lutz, A. L. Spek and G. van Koten, *J. Chem. Soc., Dalton Trans.*, 2000, 3797.
39 G. Guillena, G. Rodriguez, M. Albrecht and G. van Koten, *Chem.–Eur. J.*, 2002, **8**, 5368.
40 M. Albrecht, R. A. Gossage, A. L. Spek and G. van Koten, *Chem. Commun.*, 1998, 1003.
41 M. Albrecht, M. Schlupp, J. Bargon and G. van Koten, *Chem. Commun.*, 2001, 1874.
42 R. Hoffmann, *Acc. Chem. Res.*, 1971, **4**, 1.
43 A. Ceccon, S. Santi, L. Orian and A. Bisello, *Coord. Chem. Rev.*, 2004, **248**, 683.
44 It might be counter-intuitive to describe the attack of SO_2 on a positively charged platinum center as "electrophilic".
45 According to the DMA analysis, q^1(Pt) is much higher in $[\mathbf{1}(SO_2)]$ than in **1** (0.482 *vs.* 0.169, respectively), whereas q^1(S) and q^1(O) are very similar in $[\mathbf{1}(SO_2)]$ compared to free SO_2.
46 During the whole discussion the convention used is that the dipole moment point towards the positive charge.
47 According to a classical analysis the destabilization due to the charge–dipole interaction in $[\mathbf{2}(SO_2)]$Cl can be evaluated by $E = Q(Ru)\cdot\mu\cdot\cos\theta/R^2$, *i.e.*, 10 kJ mol^{-1} with R = 6.97 a.u., Q(Ru) = 0.0924 a.u. (NBO analysis), $\cos\theta = 1$, and $\mu = 2.05$ a.u. for $[\mathbf{1}(SO_2)]$). The corresponding calculation for $[\mathbf{4}(SO_2)]$Cl gives a value of 2 kJ mol^{-1}.

